On the structure of the generalized Poisson-Boltzmann equations

Nir Gavish[1] and Keith Promislow[2]

[1)] *Department of Mathematics, Technion – Israel Institute of Technology, Haifa, Israel*[a)]

[2)] *Michigan state University, East Lansing, MI, USA*

In this work we analyze a broad class of generalized Poisson-Boltzmann equations and reveal a common mathematical structure for this class of equations. Following our analysis we derive an explicit formula for the differential capacitance data, which enables an analytic determination of the differential capacitance data without solving the associated generalized Poisson-Boltzmann equations. Using the formula we show that differential capacitance curves generically undergo an inflection transition from a local minimum point near the point of zero charge at dilute solutions to a local maximum point for concentrated solutions. In addition, we develop a robust numerical method for solving generalized Poisson-Boltzmann equations which is easily applicable to the broad class of generalized Poisson-Boltzmann equations with very few code adjustments required for each model.

[a)] Electronic mail: ngavish@tx.technion.ac.il

I. INTRODUCTION

The contact between charged objects, such as a metal surface, macromolecule, or membrane, and an electrolyte solution results in the rearrangement of ionic distributions near the interface and formation of the so-called electrical double layer. The double layer has been extensively studied due to its importance within a wide number of areas including electrochemistry, biochemistry, physiology and colloidal science.

The Poisson-Boltzmann (PB) theory is one of the most widely used analytical method to describe double layer structure. The Poisson-Boltzmann theory is a continuum mean field-like approach assuming point-like ions immersed in a uniform dielectric medium and residing in thermodynamic equilibrium. The Poisson-Boltzmann theory does not take into account the finite-size of the ions nor their interaction among themselves and with the water molecules nearby them. As a result, the model is valid only when the charge on the interface is low and the electrolyte solution is dilute. Indeed, Poisson-Boltzmann predictions deviate from experimental data even for mildly concentrated solutions or under moderate applied voltages, see[1] for a review.

Characterization of the double layer structure in concentrated solutions or under high applied voltages is crucial to the understanding of many important systems such as fuel cells or ion channels[2,3]. The shortcomings of the Poisson-Boltzmann model have led to the development of a large family of generalized Poisson-Boltzmann equations which seek to describe the equilibrium ion profiles near a charged wall. These generalized Poisson-Boltzmann models takes into account the finite size of the ions[4–13], the dependence of the dielectric upon the electric field[14,15] or the dependence of the dielectric upon the local ionic concentration[16,17]. For a review of the different models see[1] and references within. These models were in most cases validated by differential capacitance, a measure of the overall charge imbalance in the system and one of the most important experimentally available characterization of the electric double layer. The relation between model parameters and the differential capacitance data can be determined via the solution of the associated generalized Poisson-Boltzmann equations. Accordingly, the study of each of the generalized Poisson-Boltzmann models listed above and their prediction of the differential capacitance data was based on explicit solutions when such were available, or on a numerical study using methods customized specifically for the model considered. In many cases, the numerical and analytic

study of these models focused on less-demanding symmetric cases.

In this work we show that a broad class of generalized Poisson-Boltzmann equations share a common structure that permits a considerable reduction in the limit of widely separated electrodes. In this limit the generalized Poisson-Boltzmann equations can be reduced to a dynamical system which is independent of the applied voltage, and possesses a single fixed-point, corresponding to the bulk state far from the charged plates.

Utilizing dynamical systems techniques, we derive an explicit formula for the differential capacitance that directly relates the model parameters and its differential capacitance. This formula enables an analytic determination of the differential capacitance data without solving the associated generalized PB equations. Using the formula we characterize the conditions under which differential capacitance undergoes an inflection transition from a local minimum point near the point of zero charge at dilute solutions to a local maximum point for concentrated solutions, and show that such a transition is generic.

We develop an efficient numerical scheme for solving generalized Poisson-Boltzmann equations and for computing its differential capacitance. This method is based on backward shooting from the bulk state (saddle point) toward the electrode. Utilizing the common structure of generalized Poisson-Boltzmann models, and specifically the fact that these models exhibit similar behavior near the saddle point, makes this numerical scheme easily applicable to the broad class of generalized Poisson-Boltzmann equations.

We demonstrate the numerical and analytical results by applying them to a generalized Poisson-Boltzmann model which takes into account concentration dependent dielectric[16]. To the best of our knowledge, the study of this model so far was restricted to the case of symmetric ion polarizability, probably to avoid numerical complications. The models predictions are in fair agreement between theoretical and experimental measurements in the regime of negative voltages, but not as good as agreement for positive voltages. In[16], the authors state that *"to obtain similar agreement for positive voltage, it is necessary to use a different ion polarizability, as well as two different distances of closest approach, as the ions have different effective sizes in water."* Using the dynamical systems methods, we show that taking into account the different effective sizes of ions in water indeed yields a better agreement with the theoretical and experimental results, while the data is less sensitive to ion polarizability. Moreover, at high ionic concentrations the model shows, in agreement with experiment data[18,19], that the differential capacitance undergoes an inflection transition from

a local minimum point near the point of zero charge at dilute solutions to a local maximum point for concentrated solutions.

The analytical and numerical tools presented herein allow a conceptual and numerical investigation of generalized Poisson-Boltzmann equations that encompass the impact of dielectric dependence on both electric field intensity and local ionic concentration.

Finally, the results of this paper fully address the forward problem: Given a generalized Poisson-Boltzmann equation what is its solution and what is the model's prediction for the differential capacitance data. This solution provides a solid and necessary basis for addressing the inverse problem which warrants further study: What are the classes of generalized Poisson-Boltzmann models which give rise to prescribed differential capacitance data?

II. A CLASS OF GENERALIZED POISSON-BOLTZMANN MODELS

We consider a 1:1 ionic solution bounded between two electrodes as shown in Figure 1. The walls are situated at $x = -\delta_s$ and $x = L + \delta_s$, where $\delta_s \geq 0$, with surface charge density

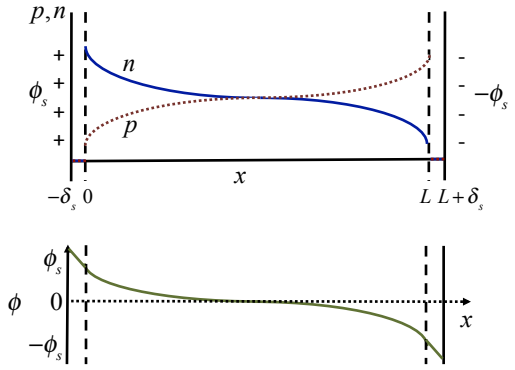

FIG. 1. Illustration of the system of study. An electrolyte solution is bounded between two oppositely charged hard walls. Top graph presents the density profiles of the cations and of the anions, denoted by $p(x)$ and $n(x)$, respectively, where a Stern layer of width δ_s near each electrode is inaccessible to charge. The bottom graph presents the potential $\phi(x)$. Much of the focus of the paper will be in the case of infinite separation length $L \to \infty$.

such that the electric potential on the walls equals,

$$\phi(-\delta_s) = \phi_s, \quad \phi(L + \delta_s) = -\phi_s, \tag{1}$$

where the reference potential is taken to be zero voltage at the bulk. The ionic densities of the cations and of the anions are described by $p(x)$ and $n(x)$, respectively. A layer of width $\delta_s \geq 0$ near each electrode is inaccessible to charge, i.e.,

$$p(x) = n(x) = 0, \quad -\delta_s < x < 0, \quad L < x < L + \delta_s.$$

The average density of anions and cations is denoted by $\overline{c}$

$$\frac{1}{L}\int_0^L p(x)\,dx = \frac{1}{L}\int_0^L n(x)\,dx = \overline{c}. \tag{2}$$

The system is globally electroneutral. Therefore, when $\phi_s = 0$, the electric field vanishes $\phi'(x) = 0$ and

$$p = n \equiv \overline{c}, \quad \phi \equiv 0, \quad \phi'(x) \equiv 0. \tag{3}$$

The solvent is described as a dielectric medium with a general dielectric response $\epsilon(I, p, n)$ which depends locally on the electric field intensity $I := (\phi')^2$ and on the ionic concentrations. In subsequent sections, we will focus on the case of infinite separation length $L \to \infty$.

A Hamiltonian describing the system outside the Stern layers[20] is given by

$$\mathcal{A}(p,n,\phi) = \int_0^L \underbrace{k_B T\left[p\left(\ln\frac{p}{\overline{c}} - 1\right) + n\left(\ln\frac{n}{\overline{c}} - 1\right)\right]}_{\text{entropy}} + \underbrace{f(p,n)}_{\text{non-Coulombic}} + \underbrace{q(p-n)\phi - \frac{1}{2}\hat{\epsilon}(I,p,n)}_{\text{electrostatic}}\,dx, \tag{4}$$

where q is the unit of electrostatic charge, k_B is Boltzmann's constant, T is the temperature. The Hamiltonian consists of the standard entropic free energy together with an additional contribution $f(p, n)$ to the energy by short-range (finite-size) interactions which can be viewed as an energetic penalty for high concentrations of ions. The last term $\hat{\epsilon}(I, p, n)$ is related to the (nonlinear) polarization of the material. The case

$$f(p,n) = 0, \quad \hat{\epsilon} = \epsilon_s I, \tag{5}$$

corresponds to the Poisson-Boltzmann free energy which does not incorporate finite-size effects and which treats the solvent as a uniform dielectric medium $\epsilon \equiv \epsilon_s$.

The double layer structures we study are critical points of the action, $\mathcal{A}$, consequently the generalized Poisson-Boltzmann equations are derived by setting the variational derivatives of $\mathcal{A}$ with respect to p, n and ϕ equal to zero, see e.g.[10] (section 2). Specifically, the variation of $\mathcal{A}$ with respect to ϕ yields a generalized Poisson equation

$$0 = \frac{\delta\mathcal{A}}{\delta\phi} = \frac{d}{dx}\left(\frac{\partial\hat{\epsilon}}{\partial I}\phi_x\right) + q(p-n) = 0, \qquad 0 < x < L, \tag{6a}$$

in which the classic permittivity (dielectric) ϵ takes the form

$$\epsilon := \frac{\partial \hat{\epsilon}}{\partial I} = -2\frac{\delta \mathcal{A}}{\delta I}.$$

Following this observation, we will restrict ourselves to functions $\hat{\epsilon}$ that satisfy

$$\frac{\partial \hat{\epsilon}}{\partial I}(I, p, n) \geq \epsilon_0, \tag{6b}$$

where ϵ_0 is the vacuum permittivity. Within the Stern layer, the dielectric constant ϵ_s is assumed to be uniform, and therefore Poisson's equation reduces to $\epsilon\phi''(x) = 0$ whose solution is linear and subject to the boundary conditions (1) equals

$$\begin{aligned} \phi(x) &= \phi_s + (x + \delta_s)\phi'(0), && 0 \leq x \leq \delta_s, \\ \phi(x) &= -\phi_s + (x - L - \delta_s)\phi'(L), && L \leq x \leq L + \delta_s. \end{aligned}$$

Accordingly, (6a) is subject to the standard Stern boundary conditions

$$\phi(0) - d\phi'(0) = \phi_s, \qquad \phi(L) + d\phi'(L) = -\phi_s. \tag{6c}$$

Similarly, setting the variation of $\mathcal{A}$ with respect to p and n equal to zero yields generalized Boltzmann equations for the charge density profiles in $0 < x < L$,

$$\begin{aligned} \lambda_p &= \frac{\delta \mathcal{A}}{\delta p} = h_p(I, p, n) + q\phi, \\ \lambda_n &= \frac{\delta \mathcal{A}}{\delta n} = h_n(I, p, n) - q\phi, \end{aligned} \tag{6d}$$

where

$$h(I, p, n) := k_B T \left[p\left(\ln \frac{p}{\overline{c}} - 1\right) + n\left(\ln \frac{n}{\overline{c}} - 1\right) + f(p, n) \right] - \frac{1}{2}\hat{\epsilon}(I, p, n), \tag{6e}$$

and λ_p and λ_n are the Lagrange multipliers associated with the conservation of mass

$$\frac{1}{L}\int_0^L p(x) - \overline{c}\, dx = 0 = \frac{1}{L}\int_0^L n(x) - \overline{c}\, dx. \tag{7}$$

For simplicity, the system (6) is non-dimensionalized by scaling

$$\tilde{\phi} = \frac{q}{k_B T}\phi, \quad \tilde{x} = \frac{x}{\lambda_D}, \quad \tilde{p} = \frac{p}{c^o}, \quad \tilde{n} = \frac{n}{c^o}, \quad \tilde{\overline{c}} = \frac{\overline{c}}{c^o}, \tag{8}$$

where λ_D is the Debye length

$$\lambda_D = \sqrt{\frac{k_B T \epsilon}{q^2 c^o}}.$$

Further, making the change of variables from ionic densities n and p to net charge density $Q = n - p$ and total mass density $\rho = n + p$, and using (3) to determining the Lagrange multipliers λ_p and λ_n yields the non-dimensional system (written after dropping the tildes)

$$\frac{d}{dx}\left[\frac{\partial \hat{\epsilon}}{\partial I}(\rho, Q, I)\phi'(x)\right] = Q, \tag{9a}$$

$$\begin{aligned} h_\rho(\rho, Q, I) &= h_\rho(2\bar{c}, 0, 0), \\ h_Q(\rho, Q, I) &= \phi + h_Q(2\bar{c}, 0, 0), \end{aligned} \tag{9b}$$

subject to boundary conditions

$$\phi(0) - \delta_s \phi'(0) = \phi_s, \qquad \phi(L) + \delta_s \phi'(L) = -\phi_s. \tag{9c}$$

Typically, the reference density c^o in (8) is set as the bulk density $\bar{c}$. Such a choice would eliminate the explicit dependence of (9) in $\bar{c}$. We choose, instead, an arbitrary reference density as a central role is played by the relationship which connects the bulk density $\bar{c}$ to the Lagrange multipliers. Additionally, after the scaling the bound(6b) takes the form

$$\hat{\epsilon}_I \geq 1. \tag{10}$$

III. COMMON STRUCTURE OF GENERALIZED POISSON-BOLTZMANNS MODELS

The system (9) is well-defined only when equation (9b) uniquely defines $\rho(\phi, I, \bar{c})$ and $Q(\phi, I, \bar{c})$. The following Lemma shows that this occurs if $h(\rho, Q)$ is strictly convex:

Lemma 1. *Equations* (9b) *uniquely define the functions* $\rho(\phi, I, \bar{c})$ *and* $Q(\phi, I, \bar{c})$ *if* $h(\rho, Q, I)$ *is a strictly convex function in* (ρ, Q) *in the domain* $\rho > 0$.

Proof. Let us rewrite equations (9b) as

$$\begin{aligned} F(\rho, Q, \phi, I) &:= h_\rho(\rho, Q, I) - h_\rho(2\bar{c}, 0, 0) = 0, \\ G(\rho, Q, \phi, I) &:= h_Q(\rho, Q, I) - \phi - h_Q(2\bar{c}, 0, 0) = 0. \end{aligned} \tag{11}$$

By the implicit function theorem, the system (11) locally defines $\rho(\phi, \bar{c}, I)$ and $Q(\phi, \bar{c}, I)$ if the Jacobian

$$J := \frac{\partial(F, G)}{\partial(\rho, Q)} = \text{Hessian}_{\rho,Q}(h)$$

is invertible. The Jacobian equals the Hessian of h, which is a positive definite matrix since h is convex. Moreover the local solution can be extended to a global one by a usual continuation argument when h is convex. □

In what follows, we will consider only the case where system (9) is well-defined, i.e., the conditions of Lemma 1 hold. Lemma 1 implies that $Q = Q(\phi, I, \bar{c})$ and $\rho = \rho(\phi, I, \bar{c})$. The direct implication of this result is that generalized Poisson-Boltzmann systems of the form (9) can be presented as an autonomous dynamical systems. Indeed, the generalized Poisson's equation (9a) reduces to

$$\frac{\partial \hat{\epsilon}}{\partial I}\phi''(x) = Q(\phi, I, \bar{c}) - \frac{d}{dx}\left(\frac{\partial \hat{\epsilon}}{\partial I}\right)\phi'(x).$$

Setting $E := \phi'(x)$, and applying the chain rule

$$\frac{d}{dx}\left(\frac{\partial \hat{\epsilon}}{\partial I}\right) = \frac{d\phi}{dx}\frac{d}{d\phi}\left(\frac{\partial \hat{\epsilon}}{\partial I}\right) = E\frac{d}{d\phi}\left(\frac{\partial \hat{\epsilon}}{\partial I}\right),$$

yields the autonomous dynamical system

$$\frac{d}{dx}\begin{bmatrix} \phi \\ E \end{bmatrix} = \begin{bmatrix} E \\ F(\phi, E; \bar{c}), \end{bmatrix}, \tag{12}$$

where $I = E^2$ and

$$F(\phi, E; \bar{c}) = \frac{Q(\phi, I, \bar{c}) - I\frac{d}{d\phi}\hat{\epsilon}_I}{\hat{\epsilon}_I}.$$

Note that (10) ensures that the denominator of $F(\phi, E)$ is strictly positive.

The system has a fixed-point at $(0, 0)$ which is a saddle point:

Lemma 2. *Under the conditions of Lemma 1 and for any $\bar{c} > 0$ and any $L > 0$, the dynamical system* (12) *has a single fixed point at* $(0, 0)$ *which is a saddle point.*

Proof. Relations (3) implies that $Q(0, 0; \bar{c}) = 0$. The bound (10) ensures that $F(0, 0) = 0$ and therefore the point $(0, 0)$ is a fixed point of (12).

The Jacobian of the system at $(0, 0)$ is

$$J = \left.\begin{bmatrix} 0 & 1 \\ Q_\phi/\hat{\epsilon}_I & Q_E/\hat{\epsilon}_I \end{bmatrix}\right|_{(0,0)}.$$

The eigenvalues of J are given by

$$\lambda_\pm = \frac{Q_E(0,0) \pm \sqrt{Q_E^2(0,0) + 4\hat{\epsilon}_I(0,0,0)Q_\phi(0,0)}}{2\hat{\epsilon}_I(0,0,0)}, \tag{13}$$

with the corresponding eigenvectors

$$\mathbf{U}_{\pm} = \begin{bmatrix} \frac{1}{\lambda_{\pm}} \\ 1 \end{bmatrix}. \tag{14}$$

We now show that $Q_\phi > 0$ which implies, together with (10), that $\lambda_\pm$ have opposite signs and therefore that $(0,0)$ is a saddle point. Indeed, differentiating (9b) with respect to ϕ and substituting $E = 0$ yields,

$$\text{Hessian}h(0,Q,\rho) \begin{bmatrix} \rho_\phi \\ Q_\phi \end{bmatrix} = \begin{bmatrix} 0 \\ 1 \end{bmatrix}.$$

By Lemma 1, Hessian$h(0,Q,\rho)$ is positive definite. Therefore, multiplying both hands by $[\rho_\phi, Q_\phi]$ yields

$$[\rho_\phi, Q_\rho]\text{Hessian}h(0,Q,\rho) \begin{bmatrix} \rho_\phi \\ Q_\phi \end{bmatrix} = [\rho_\phi, Q_\phi] \begin{bmatrix} 0 \\ 1 \end{bmatrix} = Q_\phi > 0. \tag{15}$$

Finally we show that $(0,0)$ is the only fixed point of (12). Indeed, any fixed point of (12) must satisfy $E = 0$. Let us assume in negation that there exist an additional fixed point $(\phi^*, 0)$. Then,

$$F(\phi^*, 0) = \frac{Q(\phi^*, 0)}{\hat{\epsilon}_I} = 0.$$

Thus, by (10), $Q(\phi^*, 0) = 0$. However, relation (15) implies that $Q_\phi > 0$, and we have shown that $Q(0,0) = 0$, see (3). Thus, $Q(\phi^*, 0) = 0$ if and only if $\phi^* = 0$. □

Lemma 2 shows that the saddle point structure is unperturbed under modifications to the the action which preserve the convexity of h. From a physical point of view, the saddle point describes the bulk where $\phi \approx 0$ and $E \approx 0$. Therefore, Lemma 2 implies that generalizations of the Poisson-Boltzmann model introduce terms which may give rise to significant changes near the electrodes and yield only quantitative, but not qualitative changes, in a neighbourhood of the bulk. We will exploit this property to analyze the large class of equations (9) and develop robust numerical methods for their solution.

A solution of (9) corresponds to a trajectory in the phase plane that starts from a point (ϕ_0, E_0) on the line

$$\phi_0 - \delta_s E_0 = \phi_s, \tag{16a}$$

see boundary conditions (9c), and reaches a point (ϕ_L, E_L) on the line

$$\phi_L + \delta_s E_L = \phi_s. \tag{16b}$$

These trajectories cannot pass throughout the saddle point $(0, 0)$ as they reach the point (ϕ_L, E_L) at finite 'time' $(x = L)$. To illustrate this statement we plot such trajectories for the Poisson-Boltzmann system (5,9) with $\psi_s = 1$ and $\delta_s = 0.1$, in which case, the dynamical system (12) reduces to

$$\begin{bmatrix} \phi \\ E \end{bmatrix}' = \begin{bmatrix} E \\ \sinh(\phi) \end{bmatrix}. \tag{17}$$

Specifically, in Figure 2 we plot the trajectories of (17) corresponding to the case $L = 2$

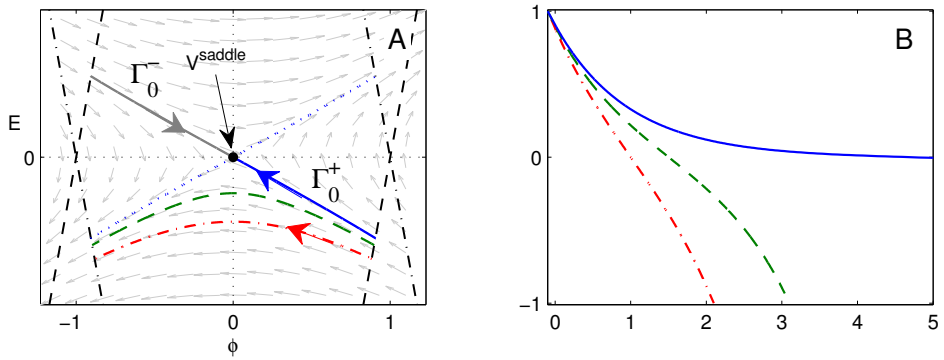

FIG. 2. A: Trajectories of the Poisson-Boltzmann dynamical system, (17) with (5) and $\delta_s = 0.1$, corresponding to $\phi_s = 1$ and $L = 2$ (dash-dotted), $L = 3$ (Dashes) and $L = \infty$ (solid). Also plotted in the trajectory Γ_0^- which corresponds to $L = \infty$ with $\phi_s = -1$, the lines $\phi - \delta_s E = \phi_s$ for $\phi_s = \pm 1$ (dashes) and the lines $\phi + \delta_s E = \phi_s$ for $\phi_s = \pm 1$ (dash-dotted) B: Solutions $\phi(x)$ of (5,17) which correspond to the three trajectories in A with $\phi_s = 1$.

(Dash-dotted) and $L = 3$ (Dashes), and their corresponding solutions. We observe that these trajectories depend on L and δ_s. Indeed, this dependence can be found explicitly, by observing that the trajectories are the graphs of $(\phi, E(\phi))$, the Dirichlet-to-Neumann map, where $E = E(\phi)$ satisfies[21]

$$E'(\phi) = \frac{F(\phi, E)}{E(\phi)}, \tag{18}$$

subject to the boundary conditions (16), and the additional constraint that

$$x(\phi_L) = \int_{\phi_0}^{\phi_L} \frac{dx}{d\phi} d\phi = \int_{\phi_0}^{\phi_L} \frac{d\phi}{E(\phi)} = L.$$

A. The limit of infinite separation length

The limit $L \to \infty$ corresponds to infinite separation length between the two electrodes. By Lemma 2, the only fixed point of (12) is $(0,0)$. Therefore, at $x \to \infty$, a trajectory can either go to the saddle point $(0,0)$ or escape toward infinity $\lim_{x\to\infty} \phi(x) = \pm\infty$. The latter option is not possible since then the mass constraint boundary condition (7) would be violated. Therefore, the trajectory in the phase plane of (12) that corresponds to the solution of generalized Poisson-Boltzmann equation in an one electrode system is the trajectory $\Gamma_0^{\pm}$ which enters the saddle from the direction $\mathbf{U}_{\pm}$, see (14). This trajectory satisfies the boundary conditions

$$\phi(0) - \delta_s \phi'(0) = \phi_s, \quad \phi(\infty) = 0, \quad E(\infty) = 0. \tag{19}$$

In addition, the mass constraints (7) reduce to

$$\rho(\infty) = 2\overline{c}, \qquad Q(\infty) = 0.$$

Accordingly, at the one-electrode setting, the system (9) reduces to the system

$$\frac{d}{dx}\left[\frac{\partial \hat{\epsilon}}{\partial I}(\rho, Q, I)\phi'(x)\right] = Q, \tag{20a}$$

$$\begin{aligned} h_\rho(\rho, Q, I) &= h_\rho(2\overline{c}, 0, 0), \\ h_Q(\rho, Q, I) &= \phi + h_Q(2\overline{c}, 0, 0), \end{aligned} \tag{20b}$$

subject to boundary conditions

$$\phi(0) - \delta_s \phi'(0) = \phi_s, \quad \phi(\infty) = 0. \tag{20c}$$

A key observation of this study is that the trajectories $\Gamma_0^{\pm}$ are independent of the value of ϕ_0 and of the value of d. The value of ϕ_0 and δ_s merely determines the part of the trajectory which is present in the region $x \in (0, \infty)$, see, e.g., Figure 3. Indeed, the trajectories leaving the saddle point $(0,0)$ are the graphs of $(\phi, E(\phi))$ where $E = E(\phi)$ satisfies, see (18),[22]

$$E'(\phi) = \frac{F(\phi, E)}{E(\phi)}, \qquad E(0) = 0. \tag{21}$$

We conclude that the boundary condition of (9) at $x = 0$ affects the dependence of $E = E(x)$ but not the form of the Dirichlet-to-Neumann map $E = E(\phi)$. From a physical point of view, the invariance of the Dirichlet-to-Neumann map implies that the electric potential and ionic

density profiles will not change if one shifts the charged wall from $x = 0$ to $x = x_0$ while changing the potential on the wall from $\phi(0)$ to $\phi(x_0)$. The invariance of E with respect to ϕ_0 holds only in the single planar-electrode setting. Indeed, as demonstrated in Figure 2, the critical point trajectory of (17) will depend significantly upon L, δ_s, and ϕ_0 when L is not large.

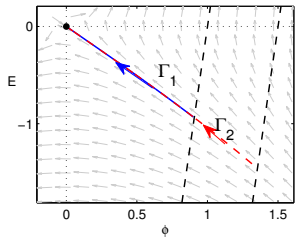

FIG. 3. A: Trajectories Γ_0 of (17) with $d = 0.1$ corresponding to $\phi_0 = 1$ (solid) and $\phi_0 = 1.5$ (dashes). Also plotted are the lines $\phi = 1 + \delta_s E$ and $\phi = 1.5 + \delta_s E$ (dashes). Changing ϕ_0 merely modifies the part of the trajectory which is present in the region $x \in (0, \infty)$.

IV. DIFFERENTIAL CAPACITANCE

The total charge imbalance in the system equals (in non-dimensional form)

$$C(\phi_s, \overline{c}) := \int_{-\delta_s}^{\infty} (p - n)\, dx.$$

The differential capacitance is defined as the change in surface charge q_s with respect to changes in the applied potential ϕ_s. Since the surface charge balances with the total charge imbalance, i.e., $q_s = -C$, we obtain

$$C_D(\phi_s, \overline{c}) := \frac{\partial q_s}{\partial \phi_s} = -\frac{\partial C}{\partial \phi_s}(\phi_s, \overline{c}).$$

Since charge imbalance occurs only in the electric double layer region, differential capacitance data provides an important indirect measurement of double layer structure.

Traditionally, the differential capacitance data predicted by a generalized PB model is computed by solving the PB equations for the charge density profiles for each desired applied voltage, integrating the spatial dependence of the charge densities, and then differentiating

the result with respect to applied voltage. The procedure is computationally inefficient and hides the underlying structure relating the generalized PB equation to the differential capacitance data.

The independence of the Dirichlet-to-Neumann map, $E(\phi, \bar{c})$ to ϕ_0, allows us to replace the boundary data ϕ_0 with the bulk value ϕ of the electric potential, and consequently derive an explicit formula for the differential capacitance. Taking into account that $Q \equiv 0$ in the Stern layer, $-d < x < 0$, and substituting the LHS of Poisson's equation (6a) in the expression for the total charge imbalance yields

$$C(\phi_s, \bar{c}) = -\int_{-\delta_s}^{\infty} Q(x; \phi_s, \bar{c})\, dx = -\int_0^{\infty} \phi_{xx}(x; \phi_s, \bar{c})\, dx = \phi_x(x; \phi_s, \bar{c})|_{x=0} = E(\phi_0(\phi_s), \bar{c}). \tag{22}$$

Thus,

$$C_D(\phi_s, \bar{c}) = -\frac{d}{d\phi_s} E(\phi_0(\phi_s), \bar{c}) = -E'(\phi_0(\phi_s))\phi_0'(\phi_s).$$

This expression can be further resolved by differentiating both sides of relation (20c) by ϕ_s to obtain

$$\phi_0'(\phi_s) - \delta_s\, E'(\phi_0, \bar{c})\phi_0'(\phi_s) = 1.$$

Isolating $\phi_0'(\phi_s)$ and substituting the result into the expression for C_D yields

$$C_D(\phi_s, \bar{c}) = \frac{-E'(\phi_0)}{1 - \delta_s E'(\phi_0)}.$$

Finally, substituting ϕ for ϕ_0, and using (21), we find the expression

$$C_D(\phi_s, \bar{c}) = \frac{-F(\phi_0, E(\phi_0), \bar{c})}{E(\phi_0) - \delta_s\, F(\phi_0, E(\phi_0), \bar{c})}. \tag{23}$$

where (ϕ_0, E_0) is the intersection point of Γ_0 with the line $\phi - \delta_s E = \phi_s$. Note that the denominator of C_D is $E - \delta_s F \neq 0$ for $F \neq 0$ since $\text{sign}(F) = -\text{sign}(E)$.

The structure of equation (23) *opens the way to a systematic analysis of the differential capacitance data*, as it defines $C_D(\phi, \bar{c})$ in terms of $E(\phi)$ without recourse to the spatial profiles $p(x), n(x)$, or $\phi(x)$. The differential capacitance data can be extracted from the PB system (9) without solving the differential equations for each value of applied voltage ϕ_0, see section V. Many of the generalized Poisson-Boltzmann models which take into account the finite size of the ions[4–13] assume a uniform dielectric $\hat{\epsilon} = \epsilon_s I$ and do not incorporate a Stern layer. In this case, equation (23) reduces to the simple form

$$C_D(\phi_s, \bar{c}) = -\frac{Q(\phi_s, \bar{c})}{E(\phi_s)}. \tag{24}$$

which relates the differential capacitance to the local ratio of the exposed charge and the electric field.

A. Inflection point

Poisson-Boltzmann theory predicts that the differential capacitance has a pronounced minimum point near the point of zero charge. Experimental measurements show double-humped or dromadary-like differential profiles, see for example Figure 4, in which the local minima lies between two local maxima. These measurements, however, were conducted for dilute solutions. More recent works have shown that in concentrated solutions[4,10,23], differential capacitance has a maximum close to the potential of zero charge, rather than the familiar minimum. These results suggest that differential capacitance data undergoes an inflection transition from local minimum at dilute solutions to a local maximum for concentrated solutions.

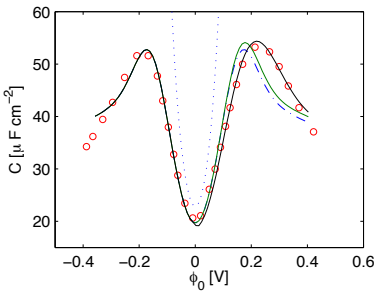

FIG. 4. Experimentally measured differential capacitance curve, taken from[24] (Figure 3) (red markers). The dotted blue curve is the prediction of the Gouy-Chapman model. The dash-dotted blue curve is the prediction by[16], equivalent to the system (20) subject to (28) with $\alpha_p = \alpha_n = -8$, and with a symmetric Stern layer of width $\delta_s = 0.48nm$. The solid green curve is the prediction of the same system with $\alpha_+ = -8$ and $\alpha_- = 3.2$, while the solid black curve results from an asymmetric Stern layer of width $\delta_s^+ = 0.48nm$ and $\delta_s^- = 0.6384nm$, and asymmetric excess polarization parameters $\alpha_+ = -8$ and $\alpha_- = 3.2$ (solid black).

Using relation (23) we can characterize the class of generalized Poisson-Boltzmann models that predicts an inflection transition in the differential capacitance. For simplicity, we provide an example of the analysis in the absence of a Stern layer, and also in symmetric

case where $f_Q \equiv 0$ and $\hat{\epsilon}_Q \equiv 0$. The symmetry assures that $\phi = 0$ is a critical point of C_D. Indeed, by relations (23) and (20b)

$$C_D'(0) = 0,$$

and

$$C_D''(0) = \frac{1}{4}\sqrt{\frac{2\overline{c}}{\hat{\epsilon}_I}}\,\frac{1 - 4\left(f_{\rho\rho} - \frac{1}{2}\hat{\epsilon}_{\rho\rho} + \frac{3\hat{\epsilon}_{I,\rho}}{2\hat{\epsilon}_I}\right)\overline{c}}{1 + 2\left(f_{\rho\rho} - \frac{1}{2}\hat{\epsilon}_{\rho\rho}\right)\overline{c}} + \frac{1}{4}\sqrt{\frac{1}{2\overline{c}}}\left(40\overline{c} - \frac{16}{3}\right)\frac{\hat{\epsilon}_{I,\phi}^2}{\hat{\epsilon}_I^{3/2}} - \frac{9\sqrt{2\overline{c}}}{4}\frac{\hat{\epsilon}_{I,\phi\phi}}{\hat{\epsilon}_I^{3/2}}. \quad (25)$$

In the primitive case, $\hat{\epsilon}_I \equiv 1$, this expression reduces to

$$C_D''(0) = \frac{\sqrt{\overline{c}}}{2\sqrt{2}}\,\frac{1 - 4f_{\rho\rho}\overline{c}}{1 + 2f_{\rho\rho}\overline{c}}.$$

Therefore, at low concentrations and under the assumption that $f_{\rho\rho}(\overline{c})$ is bounded near $\overline{c} = 0$, the differential capacitance has a local minimum at the point of zero charge since we have a local minimum point as $C_D''(0) \sim \sqrt{\overline{c}} > 0$. Conversely, if $f_{\rho\rho}(2\overline{c}, 0)\overline{c} \gg 1$ when $\overline{c} \gg 1$, then the critical point becomes a local maximum point and there is an inflection point for $\overline{c} = \overline{c}^*$ which solves

$$f_{\rho\rho}(2\overline{c}^*, 0) = \frac{1}{4\overline{c}^*}. \quad (26)$$

The Bikerman model[8], for example, corresponds to the choice of the excess free energy

$$f^{BK}(\rho) = \frac{1 - \nu\rho}{\nu}\log(1 - \nu\rho).$$

By substituting f^{BK} in (26) and solving the resulting equation for $\overline{c}^*$, we find that the Bikerman model gives rise to differential capacitance data that has an inflection point when $\overline{c}^* = \frac{1}{6\nu}$. This result can be analytically verified as an explicit expression for the differential capacitance data predicted by the Bikerman model is available and known as the Bikerman–Freise formula[1].

In Section VI, we will use expression (25) to study inflection transition in a non-primitive model where $\hat{\epsilon} = \epsilon(\rho)I$.

V. NUMERICAL METHODS

The generalized Poisson-Boltzmann system is a nonlinear boundary value problem which can be computed by an iterative process (to handle the nonlinear terms) or by forward/backward shooting. We can utilize the dynamical system presentation to efficiently

compute the solution of the generalized Poisson-Boltzmann equation by adopting a backward shooting approach. As a basis for these computations, we assume that the functions $Q(\phi, E)$ and $\rho(\phi, E)$ are known or are computed by solving (20b), and compute $E(\phi)$ by solving (21) using standard methods for computing an unstable manifold, e.g.,

Method 1 (Computation of $E(\phi)$)**.** *Given* $Q(\phi, E)$, $\rho(\phi, E)$[25] *and* $\hat{\epsilon}(Q, \rho, I)$,

1. *Set* $\phi_\delta = \text{sign}(\phi_0)\varepsilon$ *where* $0 < \varepsilon \ll 1$.

2. *Solve the initial value problem* (21) *for* $\phi \in [\phi_\delta, \phi_0]$, *with the initial condition*

$$E(\phi = \phi_\delta) = \lambda_- \phi_\delta,$$

where λ_- *is given by* (13).

The method effectively computes the trajectory Γ_0 as it leaves the saddle point. The method is stable since Γ_0 is the unstable manifold. Indeed, as illustrated in Figure 5A the distance between the trajectory Γ that corresponds to the solution of (20) and a trajectories Γ^ϵ which correspond to a backward solution with $E(\phi_\delta) = E - \varepsilon$ decreases with ϕ. Thus, we expect backward shooting to be stable for a broad class of generalized Poisson-Boltzmann equation In contrast, forward shooting would not be stable, since if the initial condition does

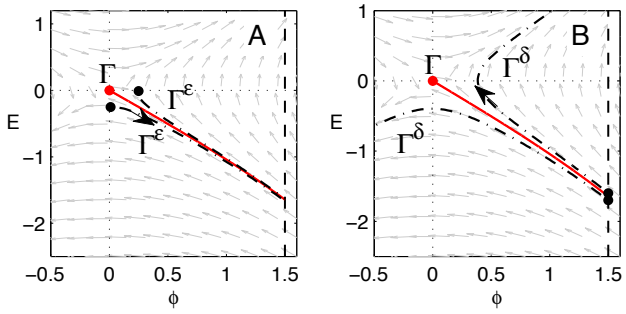

FIG. 5. The trajectory Γ that corresponds to the solution of (20). Also plotted in A: The trajectories Γ^ϵ which correspond to a backward solution with $E(L) = E_L - \varepsilon$. B: The trajectories $\Gamma^{\pm\delta}$ which correspond to a forward solution with $E(0) = E_0 \pm \delta$.

not lie exactly on the trajectory Γ, then the trajectory corresponding to the forward solution would significantly deviate from Γ near the saddle point, see, e.g., Figure 5B.

Traditionally, the differential capacitance data predicted by a generalized PB model is computed by solving the PB equations for the charge density profiles for each desired applied voltage, integrating the spatial dependence of the charge densities, and then differentiating the result with respect to applied voltage. The procedure is computationally inefficient and hides the underlying structure relating the generalized PB equation to the differential capacitance data. Using (23), the computation of the differential capacitance $C_D(\phi)$ become straightforward once $E(\phi)$ is known:

Method 2 (Computation of $C_D(\phi)$)**.**

1. *Compute $E(\phi)$ using Method 1.*

2. *Compute $\phi(0;\phi_s)$ by solving the Algebraic equation*

$$\phi(0;\phi_s) - dE(\phi(0;\phi_s)) = \phi_s,$$

   for each ϕ_s.

3. *Compute $C_D(\phi_s,\bar{c})$ by direct substitution of $E(\phi)$ and $\phi(0;\phi_s)$ in* (23)*.*

$$C_D(\phi_s,\bar{c}) = \frac{-F(\phi(0;\phi_s),E(\phi(0;\phi_s)),\bar{c})}{E(\phi(0;\phi_s)) - d\,F(\phi(0;\phi_s),E(\phi(0;\phi_s)),\bar{c})}.$$

In the absence of a Stern layer, the computation of C_D reduces to direct substitution of $E(\phi)$ in (24).

Backward shooting can also be used for computing the spatial profiles.

Method 3 (Computation of spatial profiles)**.** *Given ϕ_0, $\bar{c}$ and $Q(\phi,E,\bar{c})$,*

1. *Set location of numerical boundary at $x = L$.*

2. *Compute $\phi(x)$ by solving the system* (12) *for $x < L$ with the initial condition*

$$\phi(L) = \phi_L, \quad \phi_x(L) = E_L, \quad 0 \le x \le L$$

   where E_L is the (possibly approximate) solution of

$$\frac{\partial\hat{\epsilon}}{\partial I}(\phi_L, E_L^2)E_L = \int_0^{\phi_L} \frac{F(s;\bar{c})}{E(s;\bar{c})}ds, \tag{27}$$

and ϕ_L is found by shooting so that the ODE solution satisfies $\phi(0) = \phi_0$.

3. If needed, compute $E(x)$ by direct substitution

$$E(x) = E(\phi(x)).$$

4. Compute $Q(x, \bar{c})$ and $\rho(x, \bar{c})$ by direct substitution

$$Q(x, \bar{c}) = Q(\phi(x), \bar{c}), \qquad \rho(x, \bar{c}) = \rho(\phi(x), \bar{c})$$

As in the methods above, method 3 also involves solving an initial value problem and therefore can be computed by standard ODE solvers. Note, in addition, that it is possible to avoid solving the nonlinear integro-algebraic equation (27) for E_L, by obtaining an approximate solution for $\phi_L \ll 1$. Indeed, we have, for $0 < |\phi_L| \ll 1$,

$$\int_0^{\phi_L} \frac{Q(s;\bar{c})}{E(s;\bar{c})} ds \approx \frac{\phi_L Q(\phi_L)}{2E(\phi_L)}.$$

Thus, equation (27) reduces to

$$2\frac{\partial \hat{\epsilon}}{\partial I}(\phi_L, |E_L|^2) E_L^2 = \phi_L Q(\phi_L),$$

and the solution is chosen such that $\text{sign}(E_L) = \text{sign}(\phi_L)$.

The method computes the trajectory Γ_0 as it leaves the saddle point, different from method 1 only in the parametrization of the trajectory. As in Method 1 and as illustrated in Figure 5, we expect backward shooting to be stable for a broad class of generalized Poisson-Boltzmann equations.

VI. EXAMPLE: MODEL WITH CONCENTRATION DEPENDENT DIELECTRIC

Recent work of Hatlo et al[16] considered the generalized Poisson-Boltzmann system (20) with

$$\hat{\epsilon} = (\epsilon_w + \alpha_p p + \alpha_n n) I, \tag{28}$$

where typically $\alpha_p, \alpha_n < 0$.[26] This choice of $\varepsilon(p, n)$ reflects the observation that typically ions reduce the dielectric of the solution in their vicinity. The case $\alpha_p = \alpha_n = 0$ reduces to the Poisson-Boltzmann case. The work[16] considered only the symmetric case $\alpha_p = \alpha_n$, possibly

to avoid numerical complications. The model was validated using differential capacitance data, and achieved a fair agreement between theoretical and experimental predictions, primarily for negative voltages, see dash-dotted curve in Figure 4. In this paper, the authors state that *" to obtain similar agreement for positive voltage, it is necessary to use a different ion polarizability, as well as two different distances of closest approach, as the ions have different effective sizes in water."* Our numerical study shows that taking into account these asymmetries, indeed, yields a better agreement between theoretical and experimental results, see solid black curve in Figure 4. Furthermore, we observe that the differential capacitance data is more sensitive to changes in Stern layer width than to ion polarizability, see solid green curve in Figure 4.

Further analysis of the differential capacitance curve in the symmetric case $\alpha := \alpha_p = \alpha_n$ can be conducted by studying relation (25) for $C_D''(0)$, for which it takes the simplified form

$$C_D''(0) = \frac{1}{4}\sqrt{\frac{2\bar{c}}{\hat{\epsilon}_I^3}}\left[\hat{\epsilon}_I - 6\alpha\bar{c} - 9\alpha\rho_{\phi\phi}\right].$$

As in Section IV A, we find that the critical point in C_D changes from a local minimum to a local maximum as $\bar{c}$ increases through a critical value, all other effects held constant. This is depicted for the symmetric case in Figure 6A and for the antisymmetric case in Figure 6B.

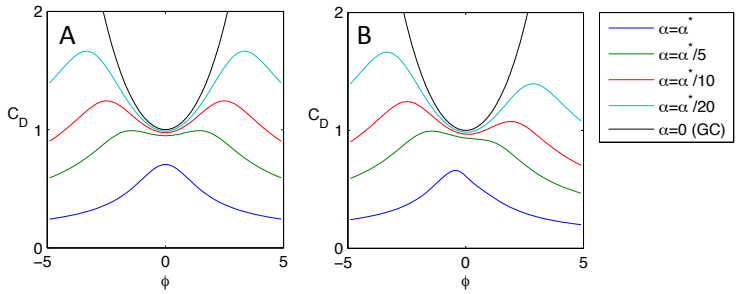

FIG. 6. Differential capacitance curves computed for solutions of (9) with concentration dependent dielectric (28) for $\bar{c} = \frac{1}{2}$ and for different values of α where A: symmetric case $\alpha_p = \alpha_n = \alpha$. B: asymmetric case, $\alpha_n = \alpha = 2\alpha_p$.

The study presented above did not require solving the generalized Poisson-Boltzmann system (20) with (28). Using backward shooting, we can solve the generalized Poisson-Boltzmann system for the spatial profiles, see Figure 7. In particular, Figure 7C presents

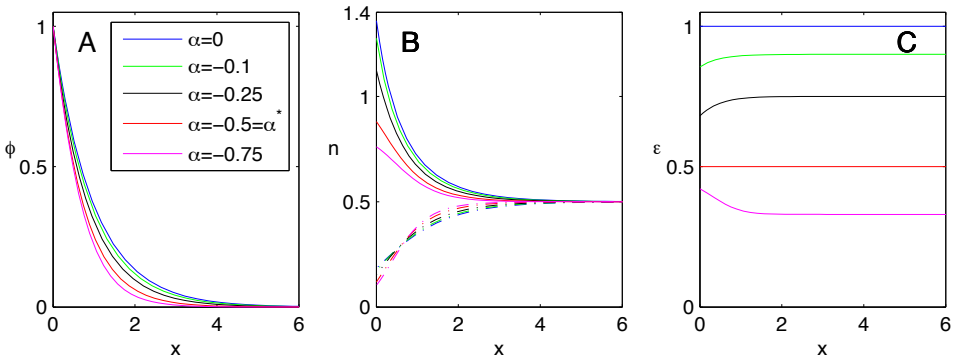

FIG. 7. Solutions of (9) with concentration dependent dielectric (28) for $\bar{c} = \frac{1}{2}$, $\phi_0 = 1$ and with different values of α. A: Electric potential ϕ. B: Concentration of negative ions n (solid curves) and positive ions p (dash-dotted curves). C: Dielectric $\varepsilon(p, n)$.

the dielectric profile which reflects the balance of two effects: the attraction of the ions towards the oppositely charged plate and, for $\alpha < 0$ the repulsion of the ions from the plate due to their tendency to reduce the dielectric constant. For $\alpha < 0$ but sufficiently small in magnitude, the first effect dominates, and the dielectric decreases near the wall, while for sufficiently negative values of α the dielectric increases near the wall. At the border line case, the the ionic profiles arrange so that the dielectric constant is spatially constant, this occurs for

$$\alpha_p = \alpha_n = \alpha^* = -\frac{1}{4}\frac{\varepsilon_w}{\bar{c}}.$$

This behavior is depicted in Figure 7C where for $\alpha = \alpha^*$ we observe a uniform dielectric profile (compare also with[17] (Figure 5)). Values of α near α^* are reasonable in physical systems, indeed setting $\varepsilon_w = 80$, we obtain that

$$\alpha^* = -\frac{20}{\bar{c}} \quad (M^{-1}).$$

Assuming that the model is valid for $\bar{c} < 2M$, we find that the range $M < \bar{c} < 2M$ corresponds to $-20 < \alpha^* < -10$. These values are comparable with $\alpha = -17$ for H^+ and $\alpha = -11$ for Li^+, $\alpha = -8$ for K^+, used in[16] (table 1). Note that the experimental data considered in[16] was obtained for $\bar{c} = 0.01M$, for which $\alpha^* \ll \alpha$, far from the regime where monotonically decreasing or uniform dielectric profiles are observed.

Acknowledgment

The first author acknowledges support from the Technion VPR fund and from EU Marie-Curie CIG grant 2018620, while the second author acknowledges support from the NSF DMS grant 1109127 and 1409940.

REFERENCES

[1]M. Z. Bazant, M. S. Kilic, B. D. Storey, and A. Ajdari, Advances in Colloid and Interface Science **152**, 48 (2009).

[2]G.-W. Wei, Q. Zheng, Z. Chen, and K. Xia, SIAM Review **54**, 699 (2012).

[3]B. Eisenberg, Biophysical journal **104**, 1849 (2013).

[4]M. Kilic, M. Z. Bazant, and A. Ajdari, Phys. Rev. E **75**, 021502 (2007).

[5]D. Ben-Yaakov, D. Andelman, D. Harries, and R. Podgornik, J. Phys.: Condens. Matter **21**, 424106 (2009).

[6]J. J. López-García, J. Horno, and C. Grosse, Langmuir **27**, 13970 (2011).

[7]H. O. Stern-Hamburg, S. f. Electrochemie **30**, 508 (1924).

[8]J. Bikerman, Philosophical Magazine **33**, 384 (1942).

[9]D. di Caprio, Z. Borkowska, and J. Stafiej, Journal of Electroanalytical Chemistry **572**, 51 (2004).

[10]D. Di Caprio, Z. Borkowska, and J. Stafiej, Journal of Electroanalytical Chemistry **540**, 17 (2003).

[11]T. Boublík, J. Chem. Phys. **53**, 471 (1970).

[12]G. Mansoori, N. Carnahan, K. Starling, and T. Leland Jr, The Journal of Chemical Physics **54**, 1523 (1971).

[13]T.-L. Horng, T.-C. Lin, C. Liu, and B. S. Eisenberg, J. Phys. Chem. B **116**, 11422 (2012).

[14]D. Ben-Yaakov, D. Andelman, R. Podgornik, and D. Harries, Current Opinion in Colloid & Interface Science **16**, 542 (2011).

[15]F. Booth, The Journal of Chemical Physics **19**, 391 (1951).

[16]M. M. Hatlo, R. van Roij, and L. Lue, EPL **97**, 28010 (2012).

[17]D. Ben-Yaakov, D. Andelman, and R. Podgornik, J. Chem. Phys. **134**, 074705 (2011).

[18]M. V. Fedorov and A. A. Kornyshev, Chemical reviews **114**, 2978 (2014).

[19]M. M. Islam, M. T. Alam, and T. Ohsaka, The Journal of Physical Chemistry C **112**, 16568 (2008).

[20]A properly posed Hamiltonian should describe the full system without the need to separately handle the Stern layer regions, see, e.g.,[13]. However, since Stern layers are introduced in many important models we have conformed with the common practice and consider a framework which can also treat Stern layers separately. We stress that all our results are valid in the absence of Stern layers, that is when $\delta_s = 0$.

[21]Equation (21) can be acquired by dividing (12) by $E := d\phi/dx$.

[22]Note that this equation does not uniquely define $E(\phi)$ since the saddle point can be approached from two directions.

[23]A. A. Kornyshev, J. Phys. Chem. B **111**, 5545 (2007).

[24]G. Valette, J. Electroanal. Chem. **122**, 285297 (1981).

[25]The function $\rho(\phi, E)$ is introduced to the initial value problem (21) only via $\hat{\epsilon}(Q, \rho, I)$. Thus, if $\hat{\epsilon} = \hat{\epsilon}(Q, I)$, e.g., in the primitive case, there is no need to compute $\rho(\phi, E)$ in order to compute $E(\phi)$.

[26]Concurrently,[17] considered a generalized Poisson-Boltzmann system with the same dielectric response function in a solution containing only negatively changed ions.